

1 Bundle sheath chloroplast volume can
2 house sufficient Rubisco to avoid limiting C₄
3 photosynthesis during chilling
4

5 Charles P. Pignon¹, Marjorie R. Lundgren^{2,3,4}, Colin P. Osborne⁵, Stephen P. Long^{1,4}

6 ¹ University of Illinois, Carl R. Woese Institute for Genomic Biology and Departments of Crop
7 Sciences and of Plant Biology, 1206 W Gregory Drive, Urbana, IL 61801, USA.

8 ² Department of Civil and Environmental Engineering, Massachusetts Institute of Technology,
9 15 Vassar Street, Cambridge, MA 02139, USA

10 ³ Arnold Arboretum, Harvard University, 1300 Centre Street, Boston, MA 02131, USA.

11 ⁴ Lancaster Environment Centre, Lancaster University, Lancaster, LA1 4YQ, UK.

12 ⁵ Department of Animal and Plant Sciences, Alfred Denny Building, University of Sheffield,
13 Sheffield, S10 2TN, UK.

14 pignon2@illinois.edu

15 slong@illinois.edu*

16 *Corresponding. 217 244 0881; 217 417 2991

17

18 Date of submission: 05/29/18

19 Four figures (two in color in print, two in black and white), one supplementary figure (video)

20 Word count: 4261

21

22 Bundle sheath chloroplast volume can
23 house sufficient Rubisco to avoid limiting C₄
24 photosynthesis during chilling
25

26 **Opinion paper**

27 **Running title:** Chloroplast volume does not restrict C₄ photosynthesis

28 **Highlight:**

29 The volume of bundle-sheath chloroplasts available for Rubisco investment in the leaves of four
30 C₄ grasses could potentially support much greater photosynthetic activity than is typically
31 observed, even at chilling temperature.

32

33 **Abstract**

34 C₄ leaves confine Rubisco to bundle-sheath cells. Thus, the size of bundle-sheath compartments,
35 and total volume of chloroplasts within them, limits space available for Rubisco. Rubisco
36 activity limits photosynthesis at low temperatures. C₃ plants counter this limitation by increasing
37 leaf Rubisco content, yet few C₄ species do the same. Because C₃ plants usually outperform C₄
38 plants in chilling environments, it has been suggested that there is insufficient chloroplast
39 volume available in the bundle-sheath of C₄ leaves to allow such an increase in Rubisco at low
40 temperatures. We investigated this potential limitation by measuring bundle-sheath and
41 mesophyll compartment volumes and chloroplast contents, as well as leaf thickness and inter-
42 veinal distance in three C₄ *Andropogoneae* grasses: two crops (*Zea mays*, *Saccharum*
43 *officinarum*) and a wild, chilling-tolerant grass (*Miscanthus x giganteus*). A wild C₄ *Panicaceae*
44 grass (*Alloteropsis semialata*) was also included. Despite significant structural differences
45 between species, there was no evidence of increased bundle-sheath chloroplast volume per leaf
46 area available to the chilling-tolerant species, relative to the chilling-sensitive ones. Maximal
47 theoretical photosynthetic capacity of the leaf far exceeded the photosynthetic rates achieved
48 even at low temperatures. C₄ bundle-sheath cells therefore house more than enough chloroplasts
49 to avoid Rubisco limitation to photosynthesis during chilling.

50

51 **Keywords:**

52 Cold tolerance, chilling tolerance, C₄ photosynthesis, confocal microscopy, chloroplast, maize,
53 *Miscanthus*, sugarcane, *Alloteropsis*, bundle-sheath

54

55 Abbreviations

- 56 A_{sat} : light-saturated net rate of photosynthetic CO₂ assimilation in leaves ($\mu\text{mol m}^{-2} \text{s}^{-1}$)
- 57 $A_{max, cp}$: A_{sat} that could be supported by the Rubisco that could be accommodated in theory within
58 the measured BS chloroplast volume ($\mu\text{mol m}^{-2} \text{s}^{-1}$)
- 59 BS: bundle-sheath
- 60 IVD : inter-veinal distance (μm)
- 61 M: mesophyll
- 62 vol_{BS} : bundle-sheath volume per unit leaf area ($\text{m}^3 \text{m}^{-2}$)
- 63 $vol_{BS, cp}$: bundle-sheath chloroplast volume per unit leaf area ($\text{m}^3 \text{m}^{-2}$)
- 64 vol_M : mesophyll volume per unit leaf area ($\text{m}^3 \text{m}^{-2}$)
- 65 $vol_{M, cp}$: mesophyll chloroplast volume per unit leaf area ($\text{m}^3 \text{m}^{-2}$)
- 66 $\%_{BS, cp}$: % occupancy of the bundle-sheath by chloroplasts (dimensionless)
- 67 $\%_{M, cp}$: % occupancy of the mesophyll by chloroplasts (dimensionless)

68 Introduction

69 C₄ photosynthesis involves a biochemical CO₂ concentrating mechanism. In mesophyll (M)
70 cells, the enzyme phosphoenolpyruvate carboxylase assimilates CO₂ into oxaloacetate, which is
71 then metabolized into further C₄ compounds that are transferred to, and decarboxylated in,
72 bundle-sheath (BS) cells to raise [CO₂] around the enzyme Rubisco (von Caemmerer and
73 Furbank, 2003). Rubisco then fixes this CO₂ via the Calvin-Benson cycle in the BS. In C₄ plants,
74 Rubisco is therefore predominantly localized to the chloroplasts of BS cells, where the increased
75 [CO₂] greatly improves photosynthetic efficiency because it effectively eliminates
76 photorespiration, the energetically costly process initiated when O₂ is fixed by Rubisco instead of
77 CO₂ (Hatch, 1987). The BS cells of C₄ leaves are arranged radially around veins and isolated
78 from internal leaf air spaces by surrounding M cells (Dengler and Nelson, 1999). Relative to the
79 leaves of C₃ plants, C₄ leaves achieve greater overall BS tissue area via a combination of higher
80 vein density, enlarged BS cells, and more numerous BS cells (Christin *et al.*, 2013; Lundgren *et*
81 *al.*, 2014).

82 The enhanced efficiency of C₄ photosynthesis under warm conditions is evident in the high
83 productivity of the *Andropogoneae* grass crops maize (*Zea mays* L.), sorghum (*Sorghum bicolor*
84 (Lu.) Moench), and sugarcane (*Saccharum officinarum* L). However, photosynthesis in the
85 majority of C₄ grasses is characterized by poor chilling tolerance, limiting them to warmer
86 environments (Long, 1983; Long and Spence, 2013; Sage, 2002). Improving chilling tolerance
87 could therefore expand the growing region and lengthen the growth seasons of C₄ crops
88 (Glowacka *et al.*, 2016). Such tolerance of low temperatures has evolved many times in wild C₄
89 grasses, enabling them to shift their niches into cooler alpine or temperate environments
90 (Watcharamongkol *et al.*, 2018).

91 The mechanisms conferring chilling tolerance to C₄ grasses have been especially well studied in
92 the grass *Miscanthus x giganteus* Greef et Deu. because of its importance for cellulosic biomass
93 production (Heaton *et al.*, 2010). For example, *Z. mays* leaves developing at 14 °C have less than
94 10% the photosynthetic capacity of *Z. mays* leaves developing at 25 °C, while leaves of *M. x*
95 *giganteus* are unaffected by this temperature difference (Long and Spence, 2013). Another study
96 found that *M. x giganteus* achieved 59% greater biomass than *Z. mays* by producing
97 photosynthetically competent leaves earlier in the year and maintaining them several weeks after

98 *Z. mays* senesced in side-by-side trials in the US corn-belt (Dohleman and Long, 2009). This
99 growth advantage may be even more pronounced in the near future, as anthropogenic climate
100 change may cause more frequent and intense springtime chilling events across the US corn-belt
101 (Kim *et al.*, 2017). Understanding and harnessing the potential of chilling-tolerant C₄
102 photosynthesis could provide crucial improvements to the yield and robustness of key C₄ crops
103 (Long *et al.*, 2006; Yin and Struik, 2017; Zhu *et al.*, 2010).

104 Chilling tolerance in C₄ grasses may be linked to leaf anatomy. Because C₄ leaves restrict
105 Rubisco to BS cells, the space potentially available to house this enzyme is roughly halved
106 relative to C₃ leaves, which can accommodate the enzyme in all photosynthetic cells (Pittermann
107 and Sage, 2000). Under moderate temperatures, flux analysis points to Rubisco as a major
108 control point on the rate of CO₂ assimilation in C₄ leaves, as it is in C₃ leaves (Furbank *et al.*,
109 1997). Since catalytic rate declines with temperature, Rubisco becomes an even greater
110 limitation under chilling, unless its amount is increased (Long and Spence, 2013; Sage *et al.*,
111 2011).

112 It has been proposed that BS chloroplast volume would limit acclimatory increases in Rubisco in
113 C₄ plants at chilling temperatures (<15 °C), so disadvantaging them relative to their C₃
114 counterparts (Kubien and Sage, 2004; Kubien *et al.*, 2003; Pittermann and Sage, 2000; Sage *et*
115 *al.*, 2011; Sage and McKown, 2006). This hypothesis is supported by the observation that leaves
116 of chilling tolerant C₃ plants often increase Rubisco content during acclimation, whereas this is
117 rarely seen in C₄ leaves (Long and Spence, 2013; Sage and McKown, 2006). Net photosynthetic
118 CO₂ uptake (A_{sat}) in C₄ leaves correlates with Rubisco content (Pearcy, 1977) and activity
119 (Friesen and Sage, 2016; Kubien and Sage, 2004; Pittermann and Sage, 2000) at low (<15 °C),
120 but not high (>25 °C), temperatures. Rubisco's flux control coefficient over photosynthetic CO₂
121 assimilation reaches 0.99 (*i.e.* near-total control) at 6 °C in *Flaveria bidentis* L. Kuntze (Kubien
122 *et al.*, 2003). These observations raise important questions: does Rubisco limit photosynthesis in
123 all C₄ plants at low temperatures, and is this limitation specifically imposed by the restricted
124 space available in the BS to house the enzyme?

125 Under chilling conditions, the chilling-tolerant *M. x giganteus* maintains photosynthetic capacity
126 and, unusually, maintains or slightly increases leaf Rubisco content per unit leaf area, while
127 showing large increases in PPDK expression (Long and Spence, 2013; Naidu *et al.*, 2003; Wang

128 *et al.*, 2008b). Accessions of *M. sacchariflorus*, one of the parent species of *M. x giganteus*,
129 achieved some of the highest light-saturated rates of leaf CO₂ uptake ($A_{sat} > 16 \mu\text{mol m}^{-2} \text{s}^{-1}$)
130 recorded for any plants grown and measured at 15 °C (Glowacka *et al.*, 2015), showing that this
131 species must accumulate sufficient Rubisco to support such high photosynthetic rates. Of
132 course, there is the possibility that these *Miscanthus* genotypes are exceptional in providing
133 unusually large bundle sheath chloroplast volumes.

134 Coinciding with the acclimation of C₄ cycle enzymes in *Miscanthus*, the upregulation of key
135 photoprotective mechanisms reduces damage to photosystem II (Farage *et al.*, 2006). This
136 suggests that decreased photosynthetic rates in most C₄ grasses at low temperature have multiple
137 causes rather than arising from one inherent limitation. Indeed, comparative transcriptomics has
138 suggested that the chilling tolerance of photosynthesis in *M. x giganteus* corresponds to the up-
139 regulation of genes encoding several photosynthetic proteins (Spence *et al.*, 2014). *M. x*
140 *giganteus* maintains the linear relationship between operating photochemical efficiency of
141 photosystem II and the quantum efficiency of CO₂ assimilation during chilling, suggesting that
142 the balance of C₃ and C₄ cycles is not compromised (Naidu and Long, 2004). In total, these
143 findings suggest that Rubisco is not the sole limitation to C₄ photosynthesis at chilling
144 temperatures, and that any volume limitation imposed by restriction of the enzyme to the bundle
145 sheath can be overcome, at least in the case of *M. x giganteus* and related species (Long and
146 Spence, 2013).

147 Because most Rubisco in C₄ leaves is confined to BS chloroplasts, a measure of the total volume
148 of chloroplasts in the BS is required to determine if there is enough space available to increase
149 Rubisco content in C₄ leaves. However, most attempts at chloroplast quantification have not
150 documented 3D measurements, but rather chloroplast counts and 2D planar area (Brown and
151 Hattersley, 1989; Pyke and Leech, 1987; Stata *et al.*, 2016; Stata *et al.*, 2014). With confocal
152 laser scanning microscopy, it is possible to measure chloroplast volume directly from an
153 optically produced 3D image (Coate *et al.*, 2012; Park *et al.*, 2009). Chloroplast measurements
154 have previously been made on fixed, dehydrated samples in accordance with TEM imaging
155 procedures (Sage and Williams, 1995). While this method is adequate for relative comparisons
156 of chloroplast size and number between plant taxonomic clades or functional types (Stata *et al.*,
157 2016; Stata *et al.*, 2014), it may distort chloroplast shape and prevent accurate estimation of

158 absolute chloroplast volume *in vivo*. Cryo-sectioning and analysis of fresh plant material may
159 prevent this type of distortion.

160 To test the hypothesis that BS chloroplast volume restricts the capacity for Rubisco to the extent
161 that it would limit photosynthesis in C₄ grasses, chloroplast volume and associated leaf
162 anatomical characteristics were measured, and used to calculate the amount and activity of
163 Rubisco that could be supported on a leaf area basis. The focus of the study was on grasses of
164 the *Andropogoneae*: since *M. x giganteus* appears to escape the low temperature limitation
165 observed in most C₄ grasses, its BS chloroplast volumes were compared to two chilling-
166 intolerant crop species of the same tribe (*Z. mays*, *S. officinarum*). The unrelated, non-
167 *Andropogoneae*, non-crop and chilling-intolerant C₄ grass (*Alloteropsis semialata* J. Presl) was
168 also included in the study (Osborne *et al.*, 2008).

169

170 Materials and methods

171 Plant material

172 Measurements were taken on *Z. mays* cv. FR1064, *S. officinarum* hybrid complex cultivar cv.
173 CP88-1762, a C₄ lineage of *A. semialata* originating from South Africa (Osborne *et al.*, 2008),
174 and the “Illinois” clone of *M. x giganteus*. *M. x giganteus* was grown in the field and the other
175 species were grown in a controlled environment greenhouse, maintained between 25 and 30 °C
176 with high pressure sodium lamps ensuring an average photon flux of 450 μmol m⁻² s⁻¹ over a 12
177 hour photoperiod.

178 *M. x giganteus* was grown at the University of Illinois Agricultural Research Station farm near
179 Champaign, IL, USA (40°02’N, 5 88°14’W, 228m above sea level). Soils at this site are deep
180 Drummer/Flanagan series (a fine silty, mixed, mesic Typic Endoaquoll) with high organic matter
181 typical of the central Illinois Corn Belt. Fertilizer was not applied. As in previous studies, the
182 youngest fully expanded leaf of *M. x giganteus* plants, as judged by ligule emergence, was
183 sampled in July (Arundale *et al.*, 2014a; Arundale *et al.*, 2014b; Dohleman *et al.*, 2012; Pignon
184 *et al.*, 2017).

185 *A. semialata* and *Z. mays* seeds were germinated on moist filter paper in a growth chamber
186 maintained at 25 °C with an average photon flux of 200 μmol m⁻² s⁻¹. They were then transferred
187 to pots of soilless cultivation medium (LC1 Sunshine mix, Sun Gro Horticulture, Agawam, MA,
188 USA), with additional coarse sand and perlite mixed into pots for *A. semialata*. Single stem
189 segments of *S. officinarum* were planted directly into pots of a second soilless cultivation
190 medium (Metromix 900: SunGro Horticulture, Agawam MA). All pots were watered daily to
191 field capacity. *Z. mays* was initially fertilized with granulated fertilizer (Osmocote Plus 15/9/12,
192 The Scotts Company LLC, Marysville, OH, USA) followed by general nutrient solution (Peter’s
193 Excel 15-5-15, Everris NA Inc, Dublin OH, USA) and iron chelate supplement (Sprint 330,
194 BASF Corp. NC, USA) added to the watering regime once every week. *A. semialata* and *S.*
195 *officinarum* were fertilized with granulated fertilizer (Osmocote Classic 13/13/13, The Scotts
196 Company LLC, Marysville, OH, USA), and *A. semialata* supplemented with iron chelate (Sprint
197 330, BASF Corp.). Plants were grown until at least the fifth leaf was fully expanded, as judged
198 by ligule emergence, and the youngest fully expanded leaf was sampled.

199 Sample preparation and measurement

200 On sampling, leaves were immediately immersed in a glycol and resin based cryostat embedding
201 medium (Tissue-Tek O.C.T. Compound, Sakura Finetek, Torrance, CA, USA), which provides
202 solid sectioning support on dry ice. 40 μm transverse sections were cut (Leica CM3050 S, Leica
203 biosystems, Wetzlar, Germany) and mounted on glass slides. Slides were then immersed for 15
204 minutes in a cell membrane and wall dye solution (FM 1-43FX, Thermofisher Scientific,
205 Waltham, MA, USA), and diluted to 3.6 mM in DMSO (Thermofisher Scientific) and water, in
206 order to image cell walls. Samples were imaged with a confocal laser-scanning microscope
207 (LSM 700, Carl Zeiss AG, Oberkochen, Germany). Images were acquired through a 63x oil-
208 immersion objective (63x Plan-Apochromat, Carl Zeiss AG) for *M. x giganteus*. It was
209 determined that reduced magnification could be used to widen the field of view while still
210 providing accurate estimates of chloroplast volume. Therefore a 40x oil-immersion objective
211 (40x Plan-Apochromat, Carl Zeiss AG) was used for *Z. mays*, *S. officinarum*, and *A. semialata*.

212 The fluorescence of dye-labelled cell walls was analyzed by excitation at 555 nm, and emission
213 was detected at a bandpass of 405-630 nm. Chlorophyll was excited at 633 nm, and its
214 fluorescence emission was detected at a bandpass of 630-700 nm. Serial optical sections were
215 obtained at 1- μm depth intervals, i.e. in the z-axis (Zen software, Carl Zeiss AG). Although
216 sampling depth (8-15 μm in the z-axis) was insufficient to capture whole BS cells, each leaf
217 section contained a random sampling of cells, which avoided the risk of biasing measurements
218 due to non-homogeneous chloroplast distribution through the length of the cell.

219 A video illustrating how the delineation of BS and M compartments, and the chloroplasts within
220 them, was achieved within a 3D optical section is shown in Fig. S1. BS and M compartments
221 were identified from the fluorescence of dye-labelled cell walls, using image segmentation
222 software (IMARIS 7.0.0 software, BitPlane, inc., Zürich, Switzerland). These segments were
223 used to determine the volume of BS (vol_{BS}) and M (vol_M) per unit leaf area. The chlorophyll
224 fluorescence signal within the BS and M was then used to determine total chloroplast volume per
225 unit leaf area within each compartment ($vol_{BS, cp}$ and $vol_{M, cp}$, respectively) and the percent
226 occupancy of each compartment by chloroplasts ($\%_{BS, cp}$ and $\%_{M, cp}$, respectively). Although
227 chlorophyll fluorescence from out-of-focus planes was typically visible in individual optical
228 slices, the surface-finding algorithm of the image segmentation software was able to accurately

229 delineate chloroplast volumes when processing the overall 3D optical section. As a result,
230 individual 2D slices appear to overestimate chloroplast content of cells, but the 3D sections
231 actually used to produce measurements do not; this can be seen by comparing Fig. 1 c to Fig. S1.

232 Leaf thickness was measured in a single location per image, across the mesophyll between two
233 veins, and inter-veinal distance (*IVD*) was measured as the average distance between the centers
234 of all the adjacent vascular bundles visible in each image.

235 Calculating photosynthetic capacity

236 An important goal of this study was to determine the theoretical maximum amount of Rubisco
237 that C₄ BS chloroplasts could contain, in order to calculate the corresponding theoretical
238 maximum level of Rubisco-limited photosynthetic CO₂ uptake ($A_{max, cp}$) that could be achieved
239 by a given leaf. Calculated values for $A_{max, cp}$ could then be compared to achieved values for
240 light-saturated photosynthetic CO₂ uptake (A_{sat}). Because $A_{max, cp}$ is a measure of theoretical, and
241 not achieved, Rubisco-limited CO₂ uptake, factors such as leaf N content and incident light
242 intensity could be ignored. Instead, $A_{max, cp}$ was determined from the volume of BS chloroplasts
243 available for Rubisco investment ($vol_{BS, cp}$), the amount of Rubisco that could be contained within
244 these chloroplasts, and the carboxylation activity of Rubisco. Although there is evidence of C₄
245 subspecies of *A. semialata* expressing Rubisco in chloroplasts outside of the BS (Ueno and
246 Sentoku, 2006), here it was assumed in all species that only BS chloroplasts contained Rubisco.

247 $vol_{BS, cp}$ was determined experimentally in this study as described above. A Rubisco
248 carboxylation rate per site at 25 °C (k_{cat}) of 3.3 mol CO₂ mol sites⁻¹ s⁻¹ had been determined
249 previously for both *Z. mays* and *M. x giganteus* (Wang *et al.*, 2008a). This value was reduced by
250 15%, reflecting the Rubisco activation state at 25 °C of 85%, reported for *M. x giganteus* (Wang
251 *et al.*, 2008a). This gives an estimated carboxylation rate of 41.6 μmol CO₂ g⁻¹ Rubisco s⁻¹ at 25
252 °C. Rubisco content per unit chloroplast volume was assumed to be 2.2 x 10⁵ g Rubisco m⁻³
253 chloroplast based on measurements for M chloroplasts of several genotypes of the hexaploid
254 bread wheat *Triticum aestivum* L. (Pyke and Leech, 1987). Combining the carboxylation rate per
255 gram Rubisco calculated with a molecular weight of 540 kDA, with the grams of Rubisco per
256 unit volume of chloroplast, leads to a theoretical maximal photosynthetic rate of 9.2 mol CO₂ m⁻³
257 chloroplast s⁻¹ at 25 °C. In the results, this factor is combined with measured BS chloroplast

258 volume ($vol_{BS, cp}$) to determine the potential photosynthetic rate that could theoretically be
259 supported given the measured chloroplast volume ($A_{max, cp}$).

260 To extend this estimation to temperatures below 25 °C, an Arrhenius function was used based on
261 the activation energy (E_a) of 78 kJ mol⁻¹ determined for Rubisco in the C₄ grass *Setaria viridis*
262 (L.) P.Beauv. (Boyd *et al.*, 2015). To compare this estimation to achieved photosynthesis values,
263 the literature was reviewed to identify values for light saturated net leaf CO₂ uptake (A_{sat}) at
264 moderate and chilling temperatures in all four species: *Z. mays* (Glowacka *et al.*, 2016; Long,
265 1983; Naidu and Long, 2004; Naidu *et al.*, 2003), *S. officinarum* (Glowacka *et al.*, 2016; Spitz,
266 2015), *A. semialata* (Osborne *et al.*, 2008), and *M. x giganteus* (Friesen and Sage, 2016;
267 Glowacka *et al.*, 2014; Glowacka *et al.*, 2016; Glowacka *et al.*, 2015; Naidu and Long, 2004;
268 Naidu *et al.*, 2003; Spitz, 2015), using values measured at different temperatures and at a photon
269 flux $\geq 1000 \mu\text{mol m}^{-2} \text{s}^{-1}$.

270 [Statistical analysis](#)

271 Replication was: *Z. mays* (n=7), *S. officinarum* (n=5), *A. semialata* (n=6), and *M. x giganteus*
272 (n=6). Statistical analysis was performed on the following parameters: leaf thickness, IVD , vol_{BS} ,
273 vol_M , $vol_{BS, cp}$, $vol_{M, cp}$, $\%_{BS, cp}$, and $\%_{M, cp}$. The fixed effect of species on each parameter was
274 tested by one-way ANOVA (PROC GLM, SAS v8.02; SAS Institute Inc., Cary, NC, USA), with
275 homogeneity of variances tested by Levene and normality of residuals tested by Shapiro-Wilke
276 (PROC UNIVARIATE, SAS v8.02) at a p=0.05 threshold. A Tukey test was performed
277 alongside the ANOVA at a p=0.05 threshold in order to identify significant pairwise differences
278 between species. When no significant differences were found, the test was repeated at a p=0.1
279 threshold to reduce the risk of a type II error given the relatively low replication for each species.

280 Results

281 The average volume of chloroplasts per unit leaf area ranged from 6-10 x 10⁻⁶ m³ m⁻² in the BS
282 and 10-14 x 10⁻⁶ m³ m⁻² in the M (Fig. 1, Fig. 2, Fig. 3 e, f). There was no evidence of greater BS
283 chloroplast volume available per unit leaf area ($vol_{BS, cp}$) in the chilling-tolerant *M. x giganteus*
284 compared with the chilling sensitive species. On the contrary, *M. x giganteus* had the smallest
285 BS chloroplast volume per unit leaf area, at ca. 40% less than the wild and chilling-sensitive *A.*
286 *semialata*. Although there were no significant differences between species in vol_{BS} , significantly
287 greater occupancy of the BS by chloroplasts ($\%_{BS, cp}$) resulted in greater $vol_{BS, cp}$ overall in *A.*
288 *semialata* (Fig. 3 c, e, g).

289 Across the four study-species, chloroplasts occupied 15-30% of the BS ($\%_{BS, cp}$), and 8-14% of
290 the M ($\%_{M, cp}$) (Fig. 1, Fig. 3 g, h, Fig. S1). Between species, $\%_{BS, cp}$ and $\%_{M, cp}$ were significantly
291 greatest and lowest, respectively, in *A. semialata*. Leaf thickness ranged from 100-250 μ m, with
292 veins spaced 100-140 μ m apart on average (Fig. 1, Fig. 3 a, b). *A. semialata* leaves at ca. 225 μ m
293 were nearly twice as thick as those of *M. x giganteus* at ca. 125 μ m. The distance between veins
294 (*IVD*) in the two crops (*Z. mays* and *S. officinarum*) was ca. 40% greater than in the two wild
295 species (*M. x giganteus* and *A. semialata*) (Fig. 3 b). Across the species, the volume of M per
296 unit leaf area (vol_M) generally mirrored leaf thickness, though due to a thick epidermis the
297 significantly greater leaf thickness of *A. semialata* did not result in a substantially greater vol_M
298 (Fig. 3 d). BS volume per unit leaf area (vol_{BS}), however, was conserved across species at ca. 40
299 m³ m⁻² x 10⁻⁶ (Fig. 3 c).

300 When the maximal theoretical photosynthetic capacity of the leaf ($A_{max, cp}$) was estimated from
301 $vol_{BS, cp}$, values ranged from ca. 60-90 μ mol m⁻² s⁻¹ at 25 °C. This was substantially greater than
302 published values of light saturated net photosynthetic CO₂ uptake (A_{sat}) for these species at this
303 temperature (Fig. 4, Table SI). However, at lower temperatures A_{sat} was closer to $A_{max, cp}$, with
304 A_{sat} being 20-90% of $A_{max, cp}$ at 5 °C.

305 Discussion

306 In all four of the C₄ grass species studied here, the volume of BS per unit leaf area available for
307 Rubisco (vol_{BS}) was not a limitation for observed rates of photosynthesis, even at chilling
308 temperatures. This conclusion is based on two key findings. First, the chilling-tolerant *M. x*
309 *giganteus* (Long and Spence, 2013) has a smaller BS chloroplast volume per unit leaf area ($vol_{BS, cp}$)
310 than the chilling-sensitive C₄ grasses *S. officinarum*, *A. semialata*, and *Z. mays* (Fig. 3).
311 Second, the theoretical maximum level of Rubisco-limited photosynthetic CO₂ uptake ($A_{max, cp}$)
312 that could be achieved by each species was greater than realized levels of A_{sat} , even at chilling
313 temperatures (Fig. 4). This study focused on closely related C₄ grasses of the *Andropogoneae*
314 clade, which contain the major C₄ crops as well as candidate bioenergy crops. Even *A. semialata*,
315 which descends from a separate evolutionary lineage in the *Paniceae*, did not suffer from
316 limitation of chilling photosynthesis by vol_{BS} .

317 Several leaf structural characteristics, including leaf thickness, *IVD*, vol_M , $\%_{BS, cp}$, and $\%_{OM, cp}$,
318 varied significantly between species (Fig. 3 a, b, d, g, h). Indeed, the $vol_{BS, cp}$ was actually
319 greatest in the chilling-sensitive *A. semialata* and lowest in the chilling-tolerant *M. x giganteus*
320 (Fig. 3 e). This clearly demonstrates that $vol_{BS, cp}$ does not determine chilling tolerance in C₄
321 plants, and therefore that the volume of BS chloroplast available for leaf Rubisco investment is
322 unlikely to meaningfully restrict C₄ photosynthesis at low temperatures.

323 Based on 2D leaf profiles, the percent occupancy of the total M volume by chloroplasts varies
324 significantly between photosynthetic types and taxonomic clades of diverse C₄ plants, with an
325 average occupation of ca. 12.2% (Stata *et al.*, 2014), which is similar to the 8-14% range seen
326 here (Fig. 3 h). In various species of the eudicot genus *Flaveria* that use the NADP-ME subtype
327 of C₄ photosynthesis, chloroplasts occupied 12-18% of the total BS volume (Stata *et al.*, 2016),
328 which is somewhat lower than the range of 15-25% seen in our grasses (Fig. 3 g); this may
329 reflect differences due to taxonomy or specimen preparation. *A. semialata*, which belongs to the
330 *Paniceae* tribe, had the greatest volume of chloroplast in the BS ($\%_{BS, cp}$) (Fig. 3 g, h). This may
331 reflect the species' need to house grana in their BS chloroplasts, while the other three studied
332 grasses of the *Andropogoneae* tribe have little to no BS chloroplast grana (Ueno and Sentoku,
333 2006). *A. semialata*'s high BS chloroplast volume may also result from the very recent
334 development of C₄ anatomy in this species, which might not have evolved the faster Rubisco

335 kinetics of other, older C₄ lineages and could therefore require relatively more Rubisco in the BS
336 to compensate (Dunning *et al.*, 2017; Lundgren *et al.*, 2015).

337 While chloroplasts across the entire M tissue are available for Rubisco investment in C₃ plants,
338 there is clearly less space available in the BS tissue of C₄ leaves. However, in the M of C₃
339 species, CO₂ must diffuse from the air space to Rubisco in the chloroplast, and chloroplasts must
340 be adjacent to the cell wall to maximize mesophyll conductance to CO₂ and facilitate Rubisco
341 access to CO₂ (Evans and Loreto, 2000; Flexas *et al.*, 2008). In the BS of C₄ species, CO₂ results
342 from decarboxylation of C₄-dicarboxylates in the chloroplast or the cytosol, and the effective
343 chloroplast volume is therefore not limited by the area of wall adjacent to air space. In effect,
344 this can allow larger and more numerous chloroplasts, and may explain the greater proportion of
345 the BS cell occupied by chloroplasts, relative to M (Fig. 3 g, h).

346 The comparison of $A_{max, cp}$ to published values for A_{sat} is directly dependent on terms used to
347 calculate $A_{max, cp}$: for instance, a 20% lower value for k_{cat} will result in 20% lower $A_{max, cp}$. At
348 lower temperatures this could lead to $A_{max, cp}$ much closer to published values for A_{sat} (Fig. 4 a,
349 b). However, the values used in this study were generally conservative. In a survey of Rubisco
350 k_{cat} in 14 grasses using different subtypes of C₄ photosynthesis (Ghannoum *et al.*, 2005), all
351 seven NADP-ME grasses, and 5 of the seven NAD-ME grasses, registered values greater than,
352 and up to two times, the k_{cat} value used here; *i.e.*, 3.3 mol CO₂ mol sites⁻¹ s⁻¹ (Wang *et al.*,
353 2008a).

354 Another important term in the calculation of $A_{max, cp}$ is the Rubisco content per unit volume
355 chloroplast. Here, we used a published value of 0.41 moles Rubisco m⁻³ chloroplast, derived
356 from *T. aestivum* M chloroplasts (Pyke and Leech, 1987). This value is conservative, as it is on
357 the lower end of the 0.4-0.5 moles Rubisco m⁻³ chloroplast range predicted from measurements
358 in C₃ chloroplasts (Jensen and Bahr, 1977). Furthermore, C₄ plants generally produce larger
359 chloroplasts than C₃ plants, particularly in the BS (Brown and Hattersley, 1989; Stata *et al.*,
360 2014) and these chloroplasts likely contain more Rubisco per unit volume, since NADP-ME C₄
361 grasses, including *Z. mays*, *S. officinarum* and *M. x giganteus*, typically show few or no stacked
362 thylakoids in the BS. This arrangement leaves more space available for stroma, and therefore
363 Rubisco, by comparison to bread wheat chloroplasts (Bellasio and Griffiths, 2014; Furbank,
364 2011; Voznesenskaya *et al.*, 2006; Voznesenskaya *et al.*, 2007).

365 Despite the use of conservative terms to calculate $A_{max, cp}$, this parameter was greater than
366 published light-saturated photosynthetic rates (A_{sat}) for all four studied species (Fig. 4) (Friesen
367 and Sage, 2016; Glowacka *et al.*, 2014; Glowacka *et al.*, 2016; Glowacka *et al.*, 2015; Long,
368 1983; Naidu and Long, 2004; Naidu *et al.*, 2003; Osborne *et al.*, 2008; Spitz, 2015). This was
369 even true at low temperatures, where Rubisco has been predicted to be a strong limitation to C₄
370 photosynthesis (Kubien and Sage, 2004; Kubien *et al.*, 2003; Pearcy, 1977; Pittermann and Sage,
371 2000). Therefore, we conclude that while the quantity of Rubisco may be limiting, this is not an
372 inherent result of the smaller proportion of cells that can contain the enzyme in C₄ leaves with
373 Kranz anatomy. Further supporting our conclusion that BS chloroplast space does not limit
374 Rubisco comes from the fact that Rubisco content does increase in *M. x giganteus* on chilling
375 (Long and Spence, 2013). Additional evidence comes from a recent transgenic upregulation of
376 Rubisco content by >30% above wild type in leaves of *Z. mays* (Salesse *et al.*, 2018).

377 Based on genetic diversity, the assumed origin of the C₄ grass tribe *Andropogoneae* is tropical
378 South-east Asia (Arthan *et al.*, 2017; Hartley, 1958). Tropical origins are common across the C₄
379 grass clades (Watcharamongkol *et al.*, 2018). Radiation into temperate climates has therefore
380 involved solving the challenges of chilling and freezing temperatures faced by all tropical plants,
381 regardless of photosynthetic type, as well as any additional restrictions added by the C₄ cycle and
382 associated anatomy. The literature has already addressed these additional restrictions and the
383 evolution of chilling tolerant C₄ photosynthesis (Long, 1983; Long, 1999; Long and Spence,
384 2013).

385 Several C₄ grasses, including *Muhlenbergia glomerata* (Kubien and Sage, 2004), *Spartina*
386 *anglica* (Long *et al.*, 1975), and *Cleistogenes squarrosa* (Liu and Osborne, 2008) can achieve
387 rates of CO₂ assimilation at chilling temperatures that equal or exceed rates achieved by
388 temperate and even arctic/alpine C₃ grasses. Notably, the C₄ grass *M. x giganteus* appears
389 exceptional in its ability to acclimate its photosynthetic apparatus to chilling temperatures.
390 Comparison with the chilling-intolerant *Z. mays* suggests that chilling tolerance in *M. x*
391 *giganteus* results from its ability to maintain and increase the expression of the enzymes PPKK
392 and Rubisco, as well as increase leaf xanthophyll content, in particular zeaxanthin, to harmlessly
393 dissipate excess absorbed light energy under chilling conditions and protect photosystem II from
394 oxidative damage (reviewed: Long and Spence, 2013). Gene expression analyses suggest that

395 these increases are part of a syndrome of acclimative changes that allow efficient C₄
396 photosynthesis under chilling conditions (Spence *et al.*, 2014), and in turn the exceptional
397 productivities achieved by *M. x. giganteus* in temperate climates (Dohleman and Long, 2009).
398 Therefore, while Rubisco content clearly co-limits photosynthesis in many C₄ species under
399 chilling conditions, the findings here show that this does not directly result from restricting
400 Rubisco to the BS in C₄ grasses.

401 In conclusion, while the volume of the cells that can hold Rubisco in C₄ grass leaves is lower
402 than in their C₃ counterparts, measurements of BS chloroplast volume show that space *per se*
403 does not present a physical, and in turn intrinsic, limitation on photosynthesis at chilling
404 temperatures. Therefore, restriction of leaf Rubisco content by the volume of BS chloroplasts
405 does not inherently limit the adaptation of C₄ grasses to cold environments.

406

407 [Supplementary material](#)

408 Supplementary Figure S1: Video of the full 3D image of leaf, bundle-sheath (BS) cells,
409 mesophyll (M) cells, and chloroplasts seen in Fig. 2. The initial 3D image, collected by confocal
410 microscopy, consists of raw fluorescence data emitted by stained cell walls (green) and
411 chloroplastic photosystem II (red). The BS and M compartments are hand-delineated (blue). The
412 chloroplasts within these compartments (**bold red**) are then identified from the photosystem II
413 autofluorescence.

414

415 Acknowledgements

416 This research was funded by the UIUC Gutgsell endowment.

417

418 **References**

- 419 **Arthan W, McKain MR, Traiperm P, Welker CAD, Teisher JK, Kellogg EA.** 2017. Phylogenomics of
420 Andropogoneae (Panicoideae: Poaceae) of Mainland Southeast Asia. *Systematic Botany* **42**, 418-431.
- 421 **Arundale RA, Dohleman FG, Heaton EA, McGrath JM, Voigt TB, Long SP.** 2014a. Yields of *Miscanthus x*
422 *giganteus* and *Panicum virgatum* decline with stand age in the Midwestern USA. *Global Change Biology*
423 *Bioenergy* **6**, 1-13.
- 424 **Arundale RA, Dohleman FG, Voigt TB, Long SP.** 2014b. Nitrogen fertilization does significantly increase
425 yields of stands of *Miscanthus x giganteus* and *Panicum virgatum* in multiyear trials in Illinois. *Bioenergy*
426 *Research* **7**, 408-416.
- 427 **Bellasio C, Griffiths H.** 2014. Acclimation of C₄ metabolism to low light in mature maize leaves could
428 limit energetic losses during progressive shading in a crop canopy. *Journal of Experimental Botany* **65**,
429 3725-3736.
- 430 **Boyd RA, Gandin A, Cousins AB.** 2015. Temperature Responses of C₄ Photosynthesis: Biochemical
431 Analysis of Rubisco, Phosphoenolpyruvate Carboxylase, and Carbonic Anhydrase in *Setaria viridis*. *Plant*
432 *Physiology* **169**, 1850-1861.
- 433 **Brown RH, Hattersley PW.** 1989. Leaf anatomy of C₃-C₄ species as related to evolution of C₄
434 photosynthesis. *Plant Physiology* **91**, 1543-1550.
- 435 **Christin PA, Osborne CP, Chatelet DS, Columbus JT, Besnard G, Hodkinson TR, Garrison LM,**
436 **Vorontsova MS, Edwards EJ.** 2013. Anatomical enablers and the evolution of C₄ photosynthesis in
437 grasses. *Proceedings of the National Academy of Sciences of the United States of America* **110**, 1381-
438 1386.
- 439 **Coate JE, Luciano AK, Seralathan V, Minchew KJ, Owens TG, Doyle JJ.** 2012. Anatomical, biochemical,
440 and photosynthetic responses to recent allopolyploidy in *Glycine dolichocarpa* (Fabaceae). *American*
441 *Journal of Botany* **99**, 55-67.
- 442 **Dengler NG, Nelson T.** 1999. Leaf Structure and Development in C₄ Plants. In: Sage RF, Monson RK, eds.
443 *C₄ Plant Biology*. San Diego, CA, USA: Academic Press, 133-172.
- 444 **Dohleman FG, Heaton EA, Arundale RA, Long SP.** 2012. Seasonal dynamics of above- and below-ground
445 biomass and nitrogen partitioning in *Miscanthus x giganteus* and *Panicum virgatum* across three
446 growing seasons. *Global Change Biology Bioenergy* **4**, 534-544.
- 447 **Dohleman FG, Long SP.** 2009. More productive than maize in the Midwest: how does *Miscanthus* do it?
448 *Plant Physiology* **150**, 2104-2115.
- 449 **Dunning LT, Lundgren MR, Moreno-Villena JJ, Namaganda M, Edwards EJ, Nosil P, Osborne CP,**
450 **Christin PA.** 2017. Introgression and repeated co-option facilitated the recurrent emergence of C₄
451 photosynthesis among close relatives. *Evolution* **71**, 1541-1555.
- 452 **Evans JR, Loreto F.** 2000. Acquisition and diffusion of CO₂ in higher plant leaves. In: Leegood RC, Sharkey
453 TD, Von Caemmerer S, eds. *Photosynthesis: Physiology and Metabolism*. Dordrecht, The Netherlands:
454 Kluwer, 321-351.
- 455 **Farage PK, Blowers D, Long SP, Baker NR.** 2006. Low growth temperatures modify the efficiency of light
456 use by photosystem II for CO₂ assimilation in leaves of two chilling-tolerant C₄ species, *Cyperus longus L.*
457 and *Miscanthus x giganteus*. *Plant Cell and Environment* **29**, 720-728.
- 458 **Flexas J, Ribas-Carbo M, Diaz-Espejo A, Galmes J, Medrano H.** 2008. Mesophyll conductance to CO₂:
459 current knowledge and future prospects. *Plant Cell and Environment* **31**, 602-621.
- 460 **Friesen PC, Sage RF.** 2016. Photosynthetic responses to chilling in a chilling-tolerant and chilling-
461 sensitive *Miscanthus* hybrid. *Plant Cell and Environment* **39**, 1420-1431.
- 462 **Furbank RT.** 2011. Evolution of the C₄ photosynthetic mechanism: are there really three C₄ acid
463 decarboxylation types? *Journal of Experimental Botany* **62**, 3103-3108.

464 **Furbank RT, Chitty JA, Jenkins CLD, Taylor WC, Trevanion SJ, vonCaemmerer S, Ashton AR.** 1997.
465 Genetic manipulation of key photosynthetic enzymes in the C₄ plant *Flaveria bidentis*. Australian Journal
466 of Plant Physiology **24**, 477-485.

467 **Ghannoum O, Evans JR, Chow WS, Andrews TJ, Conroy JP, von Caemmerer S.** 2005. Faster rubisco is
468 the key to superior nitrogen-use efficiency in NADP-malic enzyme relative to NAD-malic enzyme C₄
469 grasses. Plant Physiology **137**, 638-650.

470 **Glowacka K, Adhikari S, Peng JH, Gifford J, Juvik JA, Long SP, Sacks EJ.** 2014. Variation in chilling
471 tolerance for photosynthesis and leaf extension growth among genotypes related to the C₄ grass
472 *Miscanthus x giganteus*. Journal of Experimental Botany **65**, 5267-5278.

473 **Glowacka K, Ahmed A, Sharma S, Abbott T, Comstock JC, Long SP, Sacks EJ.** 2016. Can chilling tolerance
474 of C₄ photosynthesis in Miscanthus be transferred to sugarcane? Global Change Biology Bioenergy **8**,
475 407-418.

476 **Glowacka K, Jorgensen U, Kjeldsen JB, Korup K, Spitz I, Sacks EJ, Long SP.** 2015. Can the exceptional
477 chilling tolerance of C₄ photosynthesis found in *Miscanthus x giganteus* be exceeded? Screening of a
478 novel Miscanthus Japanese germplasm collection. Annals of Botany **115**, 981-990.

479 **Hartley W.** 1958. Studies on the origin, evolution, and distribution of the Gramineae. II. The tribe
480 Paniceae. Australian Journal of Botany **6**, 343-357.

481 **Hatch MD.** 1987. C₄ photosynthesis - a unique blend of modified biochemistry, anatomy and
482 ultrastructure. Biochimica Et Biophysica Acta **895**, 81-106.

483 **Heaton EA, Dohleman FG, Miguez AF, Juvik JA, Lozovaya V, Widholm J, Zabolina OA, McIsaac GF,**
484 **David MB, Voigt TB, Boersma NN, Long SP.** 2010. Miscanthus: a promising biomass crop. In: Kader JC,
485 Delseny M, eds. *Advances in Botanical Research, Vol 56*, Vol. 56. London: Academic Press Ltd-Elsevier
486 Science Ltd, 75-137.

487 **Jensen RG, Bahr JT.** 1977. Ribulose 1,5-Bisphosphate Carboxylase-Oxygenase. Annual Review of Plant
488 Physiology and Plant Molecular Biology **28**, 379-400.

489 **Kim J-s, Kug J-s, Jeong S-j, Huntzinger DN, Michalak AM, Schwalm CR, Wei Y, Schaefer K.** 2017.
490 Reduced North American terrestrial primary productivity linked to anomalous Arctic warming. Nature
491 Geoscience, 1-6.

492 **Kubien DS, Sage RF.** 2004. Low-temperature photosynthetic performance of a C₄ grass and a co-
493 occurring C₃ grass native to high latitudes. Plant Cell and Environment **27**, 907-916.

494 **Kubien DS, von Cammerer S, Furbank RT, Sage RF.** 2003. C₄ photosynthesis at low temperature. A study
495 using transgenic plants with reduced amounts of Rubisco. Plant Physiology **132**, 1577-1585.

496 **Liu MZ, Osborne CP.** 2008. Leaf cold acclimation and freezing injury in C₃ and C₄ grasses of the
497 Mongolian Plateau. Journal of Experimental Botany **59**, 4161-4170.

498 **Long SP.** 1983. C₄ photosynthesis at low temperatures. Plant Cell and Environment **6**, 345-363.

499 **Long SP.** 1999. Environmental Responses. In: Sage RF, Monson RF, eds. *C₄ Plant Biology*. San Diego, CA:
500 Academic Press, 215-249.

501 **Long SP, Incoll LD, Woolhouse HW.** 1975. C₄ photosynthesis in plants from cool temperate regions, with
502 particular reference to *Spartina Townsendii*. Nature **257**, 622-624.

503 **Long SP, Spence AK.** 2013. Toward Cool C₄ Crops. Annual Review of Plant Biology, Vol 64 **64**, 701-722.

504 **Long SP, Zhu XG, Naidu SL, Ort DR.** 2006. Can improvement in photosynthesis increase crop yields?
505 Plant Cell and Environment **29**, 315-330.

506 **Lundgren MR, Besnard G, Ripley BS, Lehmann CER, Chatelet DS, Kynast RG, Namaganda M,**
507 **Vorontsova MS, Hall RC, Elia J, Osborne CP, Christin PA.** 2015. Photosynthetic innovation broadens the
508 niche within a single species. Ecology Letters **18**, 1021-1029.

509 **Lundgren MR, Osborne CP, Christin PA.** 2014. Deconstructing Kranz anatomy to understand C₄
510 evolution. Journal of Experimental Botany **65**, 3357-3369.

511 **Naidu SL, Long SP.** 2004. Potential mechanisms of low-temperature tolerance of C₄ photosynthesis in
512 *Miscanthus x giganteus*: an in vivo analysis. *Planta* **220**, 145-155.

513 **Naidu SL, Moose SP, Al-Shoaibi AK, Raines CA, Long SP.** 2003. Cold tolerance of C₄ photosynthesis in
514 *Miscanthus x giganteus*: Adaptation in amounts and sequence of C₄ photosynthetic enzymes. *Plant*
515 *Physiology* **132**, 1688-1697.

516 **Osborne CP, Wythe EJ, Ibrahim DG, Gilbert ME, Ripley BS.** 2008. Low temperature effects on leaf
517 physiology and survivorship in the C₃ and C₄ subspecies of *Alloteropsis semialata*. *Journal of*
518 *Experimental Botany* **59**, 1743-1754.

519 **Park J, Knoblauch M, Okita T, Edwards G.** 2009. Structural changes in the vacuole and cytoskeleton are
520 key to development of the two cytoplasmic domains supporting single-cell C₄ photosynthesis in
521 *Bienertia sinuspersici*. *Planta* **229**, 369-382.

522 **Pearcy RW.** 1977. Acclimation of photosynthetic and respiratory carbon dioxide exchange to growth
523 temperature in *Atriplex Lentiformis* (Torr.) Wats. *Plant Physiology* **59**, 795-799.

524 **Pignon CP, Jaiswal D, McGrath JM, Long SP.** 2017. Loss of photosynthetic efficiency in the shade. An
525 Achilles heel for the dense modern stands of our most productive C₄ crops? *Journal of Experimental*
526 *Botany* **68**, 335-345.

527 **Pittermann J, Sage RF.** 2000. Photosynthetic performance at low temperature of *Bouteloua gracilis* Lag.,
528 a high-altitude C₄ grass from the Rocky Mountains, USA. *Plant Cell and Environment* **23**, 811-823.

529 **Pyke KA, Leech RM.** 1987. Cellular levels of Ribulose 1,5 Biphosphate carboxylase and chloroplast
530 compartment size in wheat mesophyll cells. *Journal of Experimental Botany* **38**, 1949-1956.

531 **Sage RF.** 2002. Variation in the k_{cat} of Rubisco in C₃ and C₄ plants and some implications for
532 photosynthetic performance at high and low temperature. *Journal of Experimental Botany* **53**, 609-620.

533 **Sage RF, Kocacinar F, Kubien DS.** 2011. C₄ Photosynthesis and temperature. In: Raghavendra AS, Sage
534 RF, eds. *C₄ Photosynthesis and Related CO₂ Concentrating Mechanisms*, Vol. 32. Dordrecht, Netherlands:
535 Springer, 1-410.

536 **Sage RF, McKown AD.** 2006. Is C₄ photosynthesis less phenotypically plastic than C₃ photosynthesis?
537 *Journal of Experimental Botany* **57**, 303-317.

538 **Sage TL, Williams EG.** 1995. Structure, ultrastructure, and histochemistry of the pollen-tube pathway in
539 the milkweed *Asclepias-exaltata* L. *Sexual Plant Reproduction* **8**, 257-265.

540 **Salesse C, Sharwood R, Busch FA, Kromdijk J, Bardal V, Stern D.** 2018. Overexpression of Rubisco
541 subunits with RAF1 increases Rubisco content in maize. *Nature Plants* (**in press**).

542 **Spence AK, Boddu J, Wang DF, James B, Swaminathan K, Moose SP, Long SP.** 2014. Transcriptional
543 responses indicate maintenance of photosynthetic proteins as key to the exceptional chilling tolerance
544 of C₄ photosynthesis in *Miscanthus x giganteus*. *Journal of Experimental Botany* **65**, 3737-3747.

545 **Spitz I.** 2015. Improving C₄ photosynthetic chilling tolerance in bioenergy crops: the search for elite
546 breeding materials., University of Illinois at Urbana-Champaign.

547 **Stata M, Sage TL, Hoffmann N, Covshoff S, Wong GKS, Sage RF.** 2016. Mesophyll Chloroplast
548 Investment in C₃, C₄ and C₂ Species of the Genus *Flaveria*. *Plant and Cell Physiology* **57**, 904-918.

549 **Stata M, Sage TL, Rennie TD, Khoshravesh R, Sultmanis S, Khaikin Y, Ludwig M, Sage RF.** 2014.
550 Mesophyll cells of C₄ plants have fewer chloroplasts than those of closely related C₃ plants. *Plant Cell*
551 *and Environment* **37**, 2587-2600.

552 **Ueno O, Sentoku N.** 2006. Comparison of leaf structure and photosynthetic characteristics of C₃ and C₄
553 *Alloteropsis semialata* subspecies. *Plant Cell and Environment* **29**, 257-268.

554 **von Caemmerer S, Furbank RT.** 2003. The C₄ pathway: an efficient CO₂ pump. *Photosynthesis Research*
555 **77**, 191-207.

556 **Voznesenskaya EV, Franceschi VR, Chuong SDX, Edwards GE.** 2006. Functional characterization of
557 phosphoenolpyruvate carboxykinase-type C₄ leaf anatomy: Immuno-, cytochemical and ultrastructural
558 analyses. *Annals of Botany* **98**, 77-91.

559 **Voznesenskaya EV, Koteyeva NK, Chuong SDX, Ivanova AN, Barroca J, Craven LA, Edwards GE.** 2007.
560 Physiological, anatomical and biochemical characterisation of photosynthetic types in genus *Cleome*
561 (*Cleomaceae*). *Functional Plant Biology* **34**, 247-267.
562 **Wang D, Naidu SL, Portis AR, Jr., Moose SP, Long SP.** 2008a. Can the cold tolerance of C₄ photosynthesis
563 in *Miscanthus x giganteus* relative to *Zea mays* be explained by differences in activities and thermal
564 properties of Rubisco? *Journal of Experimental Botany* **59**, 1779-1787.
565 **Wang DF, Portis AR, Moose SP, Long SP.** 2008b. Cool C₄ photosynthesis: Pyruvate P_i dikinase expression
566 and activity corresponds to the exceptional cold tolerance of carbon assimilation in *Miscanthus x*
567 *giganteus*. *Plant Physiology* **148**, 557-567.
568 **Watcharamongkol T, Christin PA, Osborne CP.** 2018. C₄ photosynthesis evolved in warm climates but
569 promoted migration to cooler ones. *Ecology Letters* **21**, 376-383.
570 **Yin XY, Struik PC.** 2017. Can increased leaf photosynthesis be converted into higher crop mass
571 production? A simulation study for rice using the crop model GECROS. *Journal of Experimental Botany*
572 **68**, 2345-2360.
573 **Zhu XG, Long SP, Ort DR.** 2010. Improving photosynthetic efficiency for greater yield. *Annual Review of*
574 *Plant Biology*, Vol 61 **61**, 235-261.

575

576

577 Tables and Figures

578 **Figure 1.** Individual single depth slices of representative leaf cross-sections. Cell walls labeled
579 with FM 1-43FX are green. Chlorophyll fluorescence is red. The darker red bundle-sheath
580 fluorescence of *Saccharum officinarum* L., *Zea mays* L. and *Miscanthus x giganteus* Greef et
581 Deu. reflects the lower photosystem II content in the chloroplasts, which is the primary emitter
582 of chlorophyll fluorescence in the detection bandpass of 630-700 nm. The full 3D image of the
583 *Z. mays* leaf is available as a video in Figure S1.

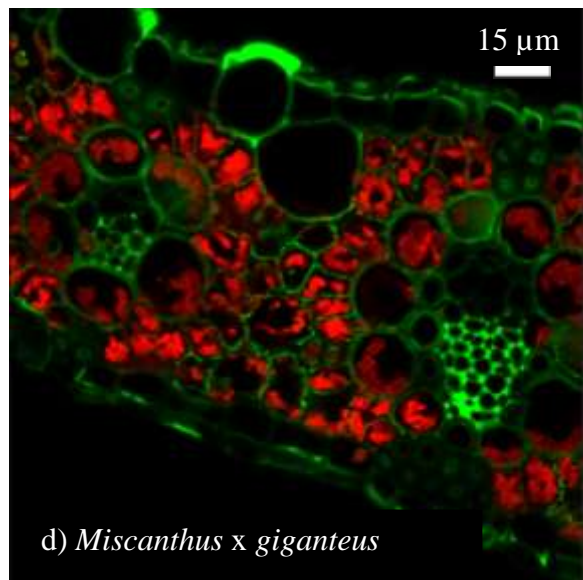
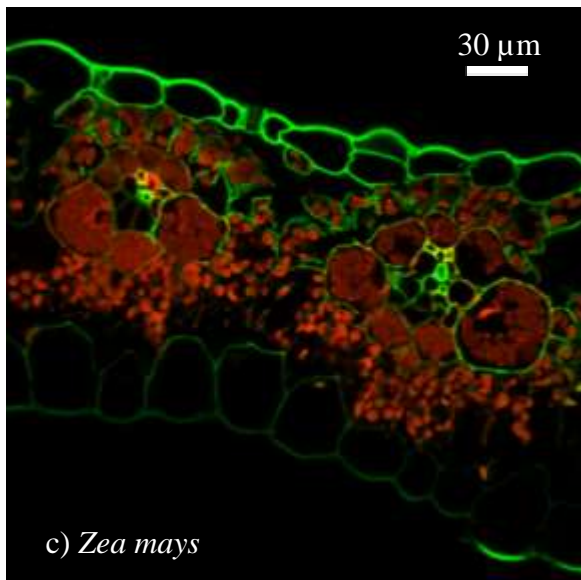
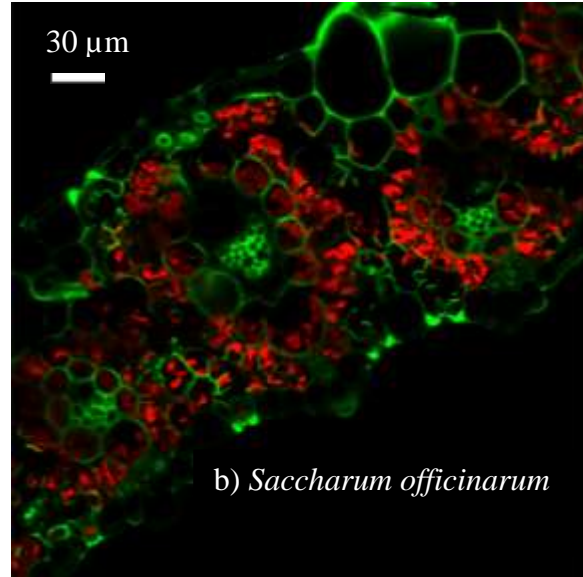
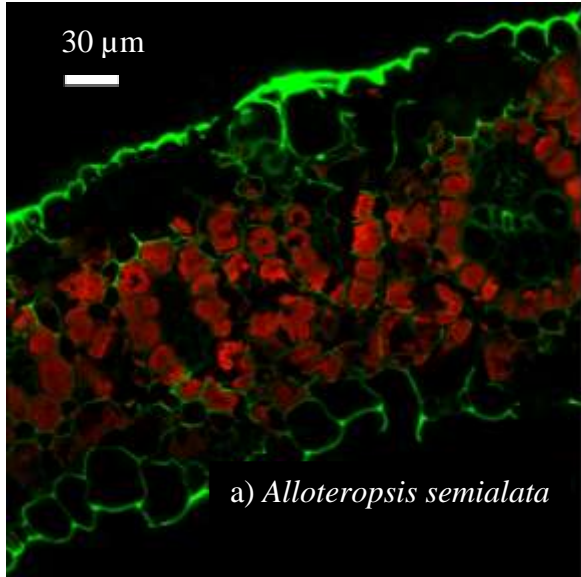
584 **Figure 2.** Fluorescent image of a representative *Zea mays* L. leaf. 2D compression of a 3D cross-
585 section of *Z. mays*, 300 μm in length and 15 μm in depth. The full 3D image is available as a
586 video in Figure S1. Cell walls labeled with FM 1-43FX are green. Chlorophyll fluorescence is
587 red. Delineated volume reconstruction of the bundle-sheath and mesophyll compartments are
588 shown in blue in panels a) and b), respectively. Chlorophyll fluorescence was used by the
589 software to reconstruct chloroplast volumes within the bundle-sheath and mesophyll; these are
590 shown in bold red in panels a) and b), respectively.

591 **Figure 3.** Leaf anatomical characteristics and differences between the study-species. Mean + SE
592 of a) leaf thickness, b) inter-veinal distance (*IVD*), c) bundle-sheath volume per leaf area (*vol_{BS}*),
593 d) mesophyll volume per leaf area (*vol_M*), e) bundle-sheath chloroplast volume per leaf area
594 (*vol_{BS, cp}*), f) mesophyll chloroplast volume per leaf area (*vol_{M, cp}*), g) occupancy of the bundle-
595 sheath by chloroplasts (*%_{BS, cp}*), and h) occupancy of the mesophyll by chloroplasts (*%_{M, cp}*) in
596 *Zea mays* L. (n=7), *Saccharum officinarum* L. (n=5), *Alloteropsis semialata* J. Presl (n=6), and
597 *Miscanthus x giganteus* Greef et Deu. (n=6). Letters indicate Tukey groups, with black letters
598 indicating significant difference at $p < 0.05$ and grey letters indicating significant difference at
599 $p < 0.1$.

600 **Figure 4.** Comparison of theoretical maximum vs. achieved leaf photosynthetic carboxylation
601 rates at different temperatures. a) Symbols indicate published rates of net CO₂ uptake (*A_{sat}*)
602 measured on leaves at different temperatures. Lines show estimated leaf maximal photosynthetic
603 capacity (*A_{max, cp}*) calculated from bundle-sheath chloroplast volume per unit leaf area. b)
604 Measurements of *A_{sat}* expressed as a percentage of *A_{max, cp}*. Measurements were obtained for *Zea*
605 *mays* L. (Glowacka *et al.*, 2016; Long, 1983; Naidu and Long, 2004; Naidu *et al.*, 2003),
606 *Saccharum officinarum* L. (Glowacka *et al.*, 2016; Spitz, 2015), *Alloteropsis semialata* J. Presl

607 (Osborne *et al.*, 2008), and *Miscanthus x giganteus* Greef et Deu. (Friesen and Sage, 2016;
608 Glowacka *et al.*, 2014; Glowacka *et al.*, 2016; Glowacka *et al.*, 2015; Naidu and Long, 2004;
609 Naidu *et al.*, 2003; Spitz, 2015) at different temperatures and at an incident photon flux ≥ 1000
610 $\mu\text{mol m}^{-2} \text{s}^{-1}$.

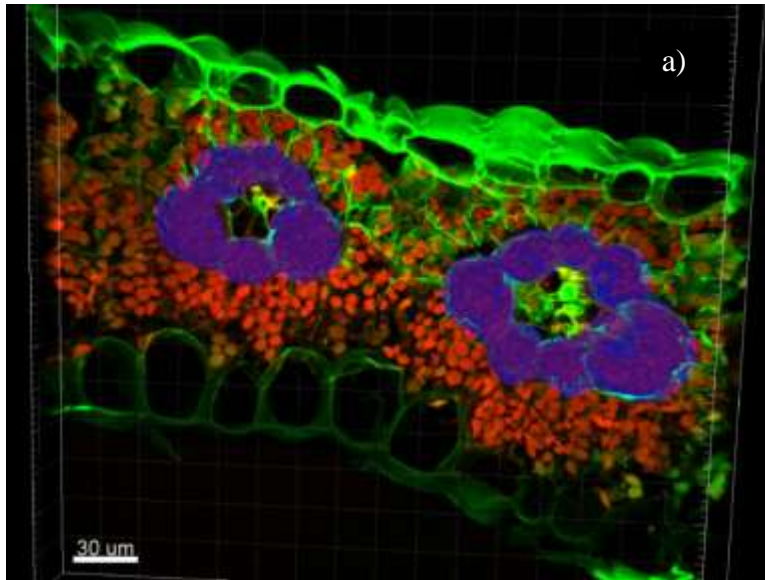
611



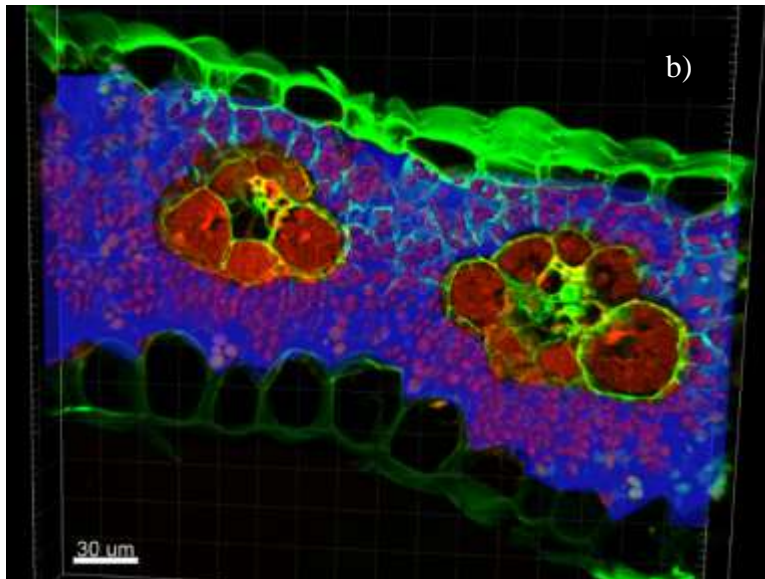
612

613 Figure 1

614



615

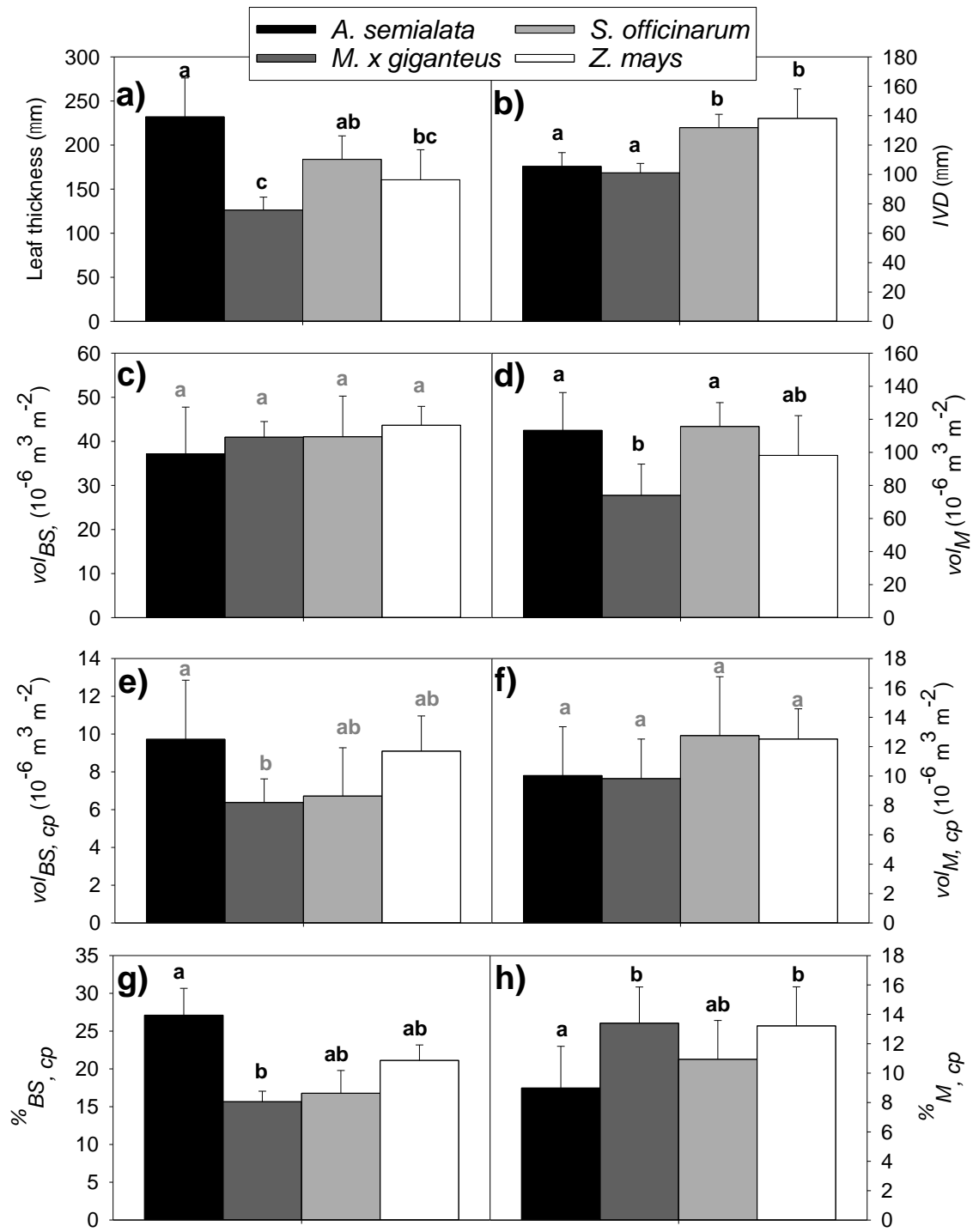


616

617 Figure 2

618

619

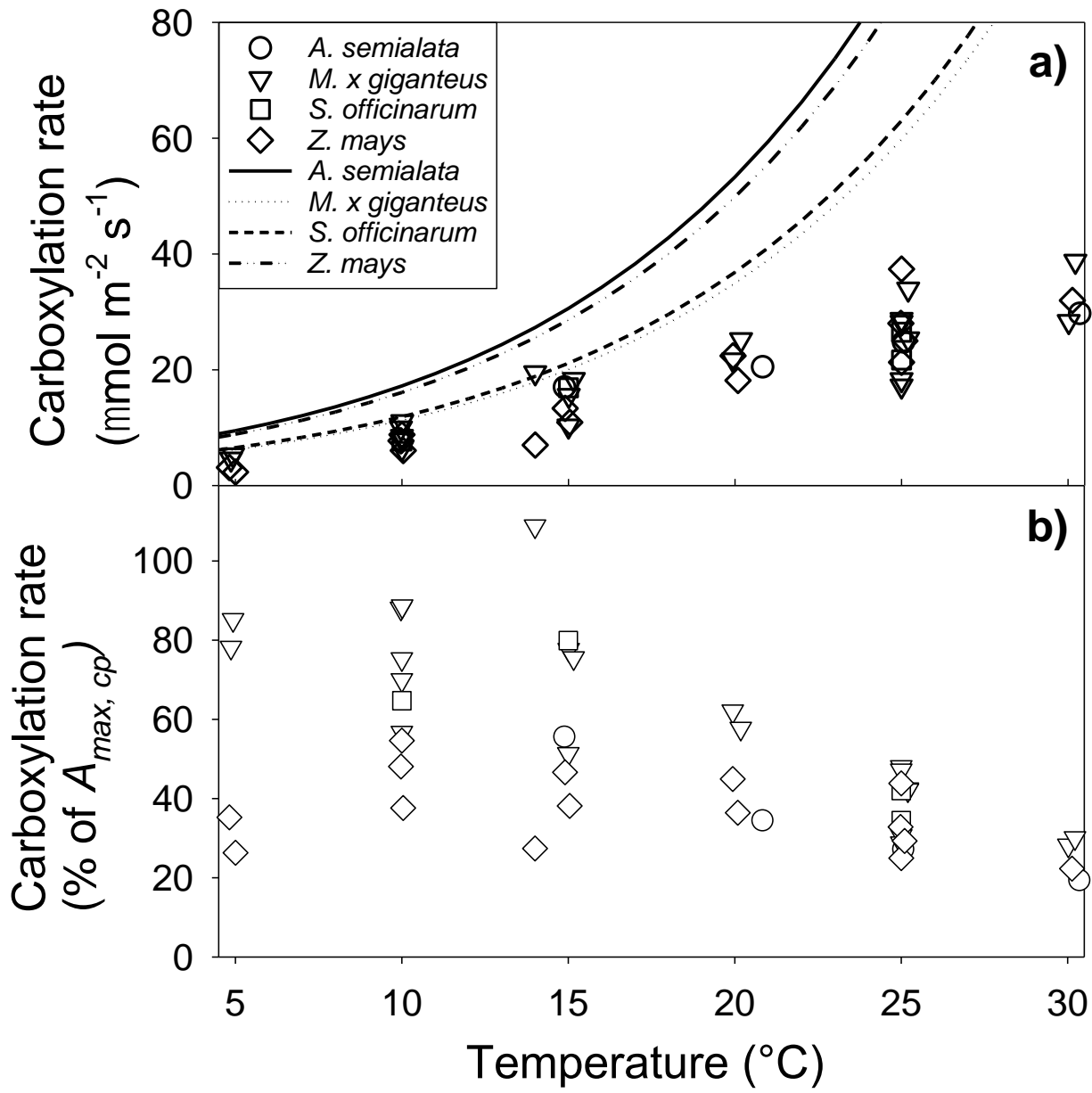


620

621 Figure 3

622

623



624

625 Figure 4